Physics

Applied Physics fields

Okayama University *Year* 2008

Preparation and characterization of epitaxial Fe2-xTixO3 films with various Ti concentrations ($0.5 < x < 1.0$)

Y. Takada* M. Nakanishi† T. Fujii‡

J. Takada** Y. Muraoka††

*Department of Applied Chemistry, Graduate School of Natural Science and Technology, Okayama University

†Department of Applied Chemistry, Graduate School of Natural Science and Technology, Okayama University

‡Department of Applied Chemistry, Graduate School of Natural Science and Technology, Okayama University, tfujii@cc.okayama-u.ac.jp

**Department of Applied Chemistry, Graduate School of Natural Science and Technology, Okayama University

††Department of Physics, Graduate School of Natural Science and Technology, Okayama University

Preparation and characterization of epitaxial $Fe_{2-x}Ti_xO_3$ films with various Ti concentrations ($0.5<x<1.0$)

Y. Takada,[1] M. Nakanishi,[1] T. Fujii,[1,a)] J. Takada,[1] and Y. Muraoka[2]
[1]*Department of Applied Chemistry, Graduate School of Natural Science and Technology, Okayama University, Tsushimanaka 3-1-1, Okayama 700-8530, Japan*
[2]*Department of Physics, Graduate School of Natural Science and Technology, Okayama University, Tsushimanaka 3-1-1, Okayama 700-8530, Japan*

(Received 25 October 2007; accepted 11 June 2008; published online 13 August 2008)

An ilmenite-hematite solid solution ($Fe_{2-x}Ti_xO_3$) is one of the candidates for practical magnetic semiconductors with a high Curie temperature. We have prepared well-crystallized epitaxial $Fe_{2-x}Ti_xO_3$ films with a wide range of Ti concentrations—x=0.50, 0.60, 0.65, 0.76, 0.87, and 0.94—on α-Al_2O_3(001) substrates. The films are prepared by a reactive helicon plasma sputtering technique to evaporate Fe and TiO targets simultaneously under optimized oxygen pressure conditions. The structural characterizations of the films reveal that all films have a single phase of the ordered structure with $R\bar{3}$ symmetry, where Ti-rich and Fe-rich layers are stacked alternately along the c axis. All films have large ferrimagnetic moments at low temperature, and room temperature magnetization is clearly observed at $x<0.7$. The inverse temperature dependence of the resistivities of the films indicates their semiconducting behavior. The film resistivities decrease with decreasing Ti concentration. © *2008 American Institute of Physics*. [DOI: 10.1063/1.2966298]

I. INTRODUCTION

Magnetic semiconductors are one of the key materials for developing future spintronics devices. Materials with a high Curie temperature (T_C) exceeding 400 °C are required for their practical use.[1] There are many approaches to produce magnetic semiconductors. Dilute magnetic semiconductors such as Mn-doped GaAs[1,2] and Co-doped TiO_2,[3] in which small amounts of magnetic ions are substitute for nonmagnetic ions of traditional semiconductors, have been investigated extensively. An alternate approach is to develop nontraditional semiconducting materials exhibiting intrinsic magnetization at room temperature. An ilmenite-hematite solid solution ($Fe_{2-x}Ti_xO_3$) is one of the candidates for nontraditional magnetic semiconductors because intermediate compositions between ilmenite ($FeTiO_3$) and hematite (α-Fe_2O_3) are known to be both semiconducting and ferrimagnetic.[4–6] A recent theoretical calculation has predicted that $Fe_{2-x}Ti_xO_3$ is a strong candidate for a magnetic semiconductor with strong spin-dependent transport properties and a high Curie temperature above 400 °C.[7–9] Moreover, a solid solution system can produce either an n-type or a p-type semiconductor by changing the Fe-to-Ti concentration ratio.[6]

Both α-Fe_2O_3 and $FeTiO_3$ are characterized by a crystal structure derived from a corundum structure such as α-Al_2O_3. The structure consists of a hexagonal close-packed oxygen array, in which cations occupy two-thirds of octahedral interstices. If all cation sites are crystallographically equivalent to α-Fe_2O_3, the structure has $R\bar{3}c$ symmetry. $FeTiO_3$ has $R\bar{3}$ symmetry, in which alternate Fe layers along the c axis are replaced by Ti. Therefore, the solid solution of $Fe_{2-x}Ti_xO_3$ has an order ($R\bar{3}$ symmetry)-disorder ($R\bar{3}c$ symmetry) transition. Only solid solutions with $R\bar{3}$ symmetry exhibit large ferromagnetic moments. Recently, Hojo *et al.* have succeeded in preparing room temperature ferrimagnetic $Fe_{1.4}Ti_{0.6}O_3$ films with $R\bar{3}$ symmetry by the pulsed laser deposition technique.[10,11] The spin polarization of n-type carriers in $Fe_{1.4}Ti_{0.6}O_3$ is clearly suggested by Hall effect measurements. We previously reported the preparation of well-crystallized epitaxial $Fe_{2-x}Ti_xO_3$ films with various Ti concentrations in the range $0.6<x<1.0$.[12–14] The films were formed on sapphire single-crystalline substrates by the reactive sputtering technique using a Fe–Ti alloy target to accurately control the oxygen partial pressure and substrate temperature. The T_C value of $Fe_{2-x}Ti_xO_3$ films increased linearly with decreasing Ti concentration. In order to extend the formation range of well-crystallized $Fe_{2-x}Ti_xO_3$ films with $R\bar{3}$ symmetry, cosputtering from Fe and TiO targets was employed for preparing $Fe_{2-x}Ti_xO_3$ films with a small Ti concentration. The cosputtering technique offers advantages such as the easy tuning of the Fe-to-Ti concentration ratio and its extensive control. In the present paper, we report the preparation of well-crystallized epitaxial $Fe_{2-x}Ti_xO_3$ films over a wide solid solution range of $0.5<x<1.0$. The structures and magnetic and electric properties of the films are examined as a function of the Ti concentration.

II. EXPERIMENTAL

$Fe_{2-x}Ti_xO_3$ films with various Ti concentrations were prepared on α-Al_2O_3(001) single-crystalline substrates by using a helicon plasma sputtering system with a base pressure of 10^{-7} Pa. The outline of our sputtering system is illustrated in Fig. 1. The system had two cathodes—one with a Fe metal target and the other with a TiO target. Before sput-

a)Electronic mail: tfujii@cc.okayama-u.ac.jp.

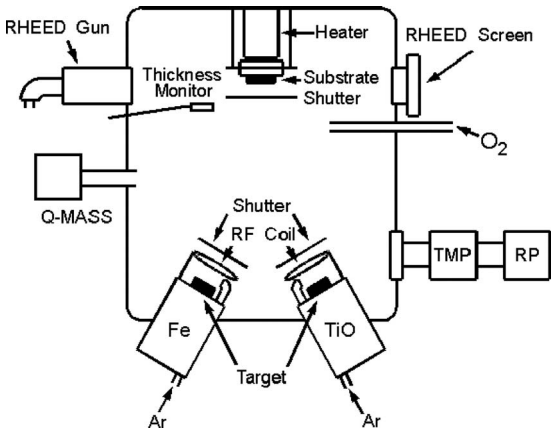

FIG. 1. Schematic illustration of helicon plasma sputtering system.

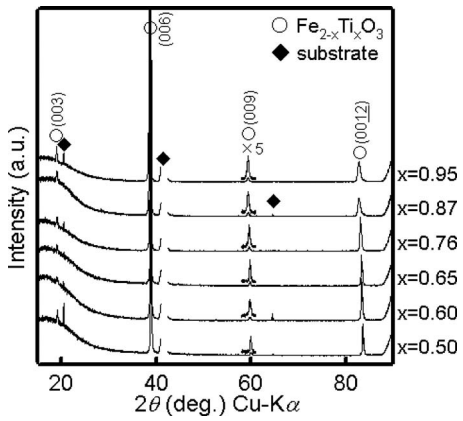

FIG. 2. XRD patterns of $Fe_{2-x}Ti_xO_3$ films as a function of Ti concentration x.

tering deposition, the substrate was annealed in vacuum at 700 °C for 1.5 h for surface cleaning. During the sputtering deposition, high-purity gases Ar (99.999%) and O_2 (99.995%) were introduced into the system with precise gas flow control. The equilibrium oxygen pressure for $Fe_{2-x}Ti_xO_3$ was strongly dependent on the Ti concentration.[15] Therefore, the oxygen partial pressure (P_{O_2}) during the sputtering deposition was monitored *in situ* by a mass analyzer unit to maintain the optimized P_{O_2} values for individual Ti concentrations. The substrate temperature was fixed to 700 °C. The Fe-to-Ti concentration ratio in the deposited films was controlled to adjust the rf sputtering powers for the Fe and TiO targets individually. All films were subsequently annealed in vacuum at 700 °C for 2 h to promote chemical ordering processes from $R\bar{3}c$ to $R\bar{3}$ symmetry.[14] The thicknesses of all sample films were fixed to 80 nm. The crystal structures of the films were characterized by the x-ray diffraction (XRD) technique using Cu $K\alpha$ radiation ($\lambda = 1.5406$ Å). Magnetization measurements were carried out using a vibrating sample magnetometer under a magnetic field applied parallel to the film plane. The electric resistivities of the films were measured between 130 and 400 K by a dc four-probe method. The electronic structures of the deposited films were examined by conversion electron Mössbauer spectroscopy (CEMS) by using a gas flow counter at room temperature. The chemical compositions of the prepared films were analyzed by energy dispersive x-ray spectroscopy (EDS).

III. RESULTS AND DISCUSSIONS

Figure 2 shows the typical XRD patterns of the deposited films with various Ti concentrations ($x=0.50$, 0.60, 0.65, 0.76, 0.87, and 0.95, analyzed by EDS). The x-ray scattering vector was aligned normal to the film plane. All films had an ilmenite structure. No secondary phase such as $Fe_{3-x}Ti_xO_4$ (spinel structure) or $Fe_{2-x}Ti_{1+x}O_5$ (pseudobrookite) was detected. The cation ordering in $Fe_{2-x}Ti_xO_3$ was reflected by the relative intensities of the XRD patterns. When all the cation sites were equivalent, the films had a corundum structure with the $R\bar{3}c$ symmetry and only two diffraction lines indexed as (006) and (00$\underline{12}$) appeared. Two additional diffraction lines indexed as (003) and (009) indicated that the ordered cation array along the c axis formed the ilmenite structure with the $R\bar{3}$ symmetry. It was confirmed that all the deposited films had the ilmenite structure. It should be noted that the $Fe_{2-x}Ti_xO_3$ films with the $R\bar{3}$ symmetry were formed on the substrate for a wide range of Ti concentrations, even at $x=0.50$. However, the intensities of the odd indexed lines, which were typical of the $R\bar{3}$ symmetry, were slightly less than the ideal value calculated from the fully ordered structure. In order to evaluate the cation ordering of the deposited $Fe_{2-x}Ti_xO_3$ films, the order parameter Q was estimated from the integrated diffraction intensity ratio between the (006) and (009) lines. $Q=0$ implies the fully disordered state with Fe and Ti ions equally distributed over the two cation sites, whereas $Q=1$ implies the fully ordered state with all Ti ions occupying only one cation site. The estimated Q values of the $Fe_{2-x}Ti_xO_3$ films were nearly constant ($Q=0.7$) for $x=0.7-1.0$ and gradually decreased with decreasing x. Incidentally, $FeTiO_3$ bulk crystals are known to have an almost fully ordered structure even after being quenched from high temperature.[16] The inferior cation ordering of the deposited films could be related to the introduced strains in the films, which is discussed later.

The out-of-plane lattice constant c of the $Fe_{2-x}Ti_xO_3$ films determined from the (006) diffraction line is shown in Fig. 3(a) as a function of the Ti concentration x. The in-plane lattice constant a was obtained from reciprocal area scans of the (104) diffraction lines. The solid lines in Fig. 3 represent the linear interpolation between the unit cell parameters of α-Fe_2O_3 and $FeTiO_3$ bulk crystals.[17] The x-ray scattering vector of the (104) lines was inclined by approximately 38.2° from the normal to the film plane and showed a clear threefold symmetry due to the multiplicity of the rhombohedral symmetry. The reciprocal area scans clearly confirmed the epitaxial growth of the $Fe_{2-x}Ti_xO_3$ films on the α-Al_2O_3(001) substrates. According to the crystal chemistry of the bulk crystals, the unit cell volume of the α-Fe_2O_3–$FeTiO_3$ solid solution system followed Vegard's law.[18] However, the c values of all films were considerably smaller than those of the bulk crystals, as predicted by Vegard's law. On the other hand, the a values of all films were larger than those of the bulk crystals, particularly for the film with $x=0.5$. It should be noted that the unit cell volumes of all the films except for

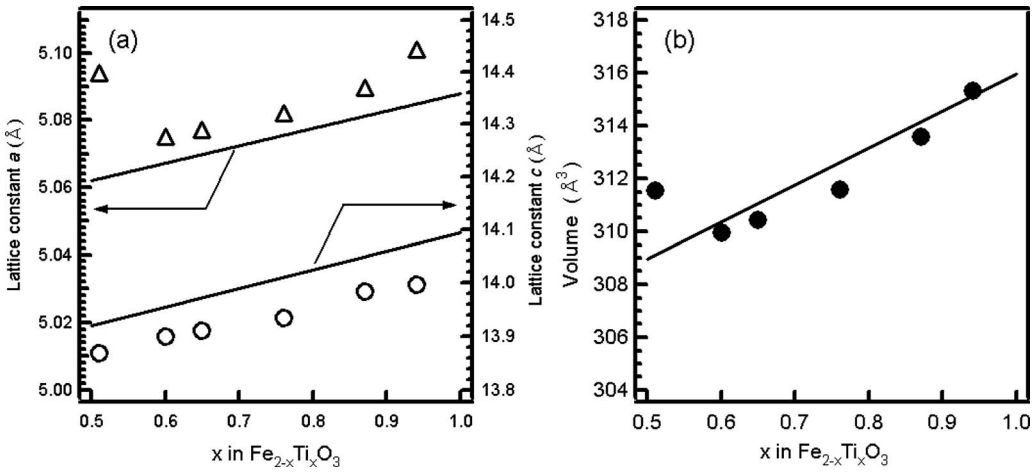

FIG. 3. x dependence of (a) lattice constants a (open triangles) and c (open circles) and (b) unit cell volume of $Fe_{2-x}Ti_xO_3$ films. The solid lines represent the linear interpolation between the unit cell parameters of α-Fe_2O_3 and $FeTiO_3$ bulk crystals, which follow Vegard's law.

the film with $x=0.5$ consequently followed Vegard's law. This result clearly suggested that the solid solution films had good oxygen stoichiometry. If oxygen nonstoichiometry was introduced into the films as $Fe_{2-x}Ti_xO_{3+\delta}$, considerable changes would be expected in the unit cell volume.[12] Further, all the films were strained by a large amount to cause tensile stress within the film plane. The cation ordering reported in the $Fe_{2-x}Ti_xO_3$ bulk crystals was such that compressive stress and tensile stress were desirable in the a axis and c axis, respectively.[16] The opposite signs of the film strains could be the cause of the inferior cation ordering of the films, as mentioned previously.

The typical magnetization curves of the $Fe_{2-x}Ti_xO_3$ films at $x=0.5$ measured at room temperature and 78 K are shown in Fig. 4. The diamagnetic contribution of the substrate was subtracted from the raw magnetization data. The magnetization curves did not saturate up to high magnetic fields (16 kOe), probably due to the presence of twin domain boundaries and/or compositional modulations in $Fe_{2-x}Ti_xO_3$.[19] Therefore, the saturation magnetization (M_S) here was defined by the magnetization values at 8.5 kOe in respect to the reference article.[4] Figure 5 shows the measured M_S values for various $Fe_{2-x}Ti_xO_3$ films as a function of the Ti concentration x. All films were ferrimagnetic at 78 K, as expected from an ordered structure with $R\bar{3}$ symmetry. Moreover, the films with $x=0.5-0.7$ exhibited spontaneous magnetization even at room temperature. The observed room temperature magnetizations for $x=0.7-0.9$ were a result of the paramagnetic response to the applied magnetic field because their magnetization curves had no hysteresis. In bulk ceramics, the magnetic ordering temperature (the Néel or Curie temperature) decreased monotonically from 950 K ($x=0$) to 55 K ($x=1.0$) through room temperature at $x\sim0.7$. The solid solution films exhibited the maximum magnetization at $x=0.76$ at 78 K. The Ti concentration at which the maximum magnetization value was obtained was consistent with that of bulk ceramics at the same temperature.[5] However, the observed magnetization M_S was slightly smaller than the experimental magnetization value of the bulk samples.[4,19] This result also suggested a slightly inferior cation ordering of the prepared films.

The electrical resistivities of the $Fe_{2-x}Ti_xO_3$ films with various Ti concentrations are shown in Fig. 6 as a function of the inverse temperature. The resistivities were measured by a constant current method with a constant current of 1.0 μA in order to prevent the nonlinear current-voltage characteristics of $Fe_{2-x}Ti_xO_3$.[20] The films clearly exhibited thermally activated semiconducting behavior, in which logarithmic resistivity varied linearly with inverse temperature. The resistivities decreased monotonically with decreasing Ti concen-

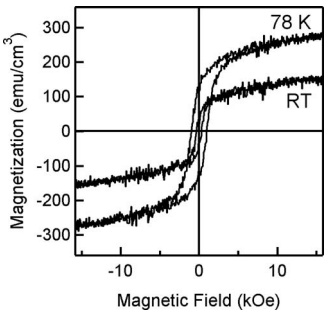

FIG. 4. Typical magnetization curves of $Fe_{2-x}Ti_xO_3$ films at $x=0.5$ measured at room temperature and 78 K.

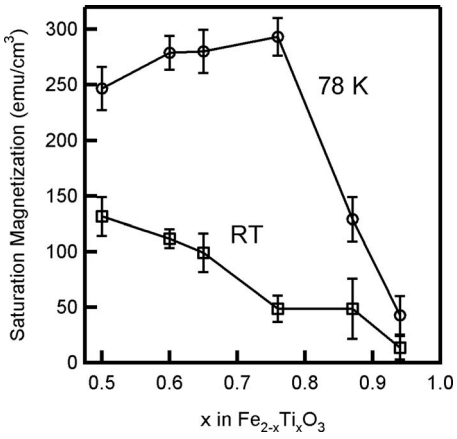

FIG. 5. Saturation magnetization of $Fe_{2-x}Ti_xO_3$ films measured at room temperature and 78 K as a function of Ti concentration x.

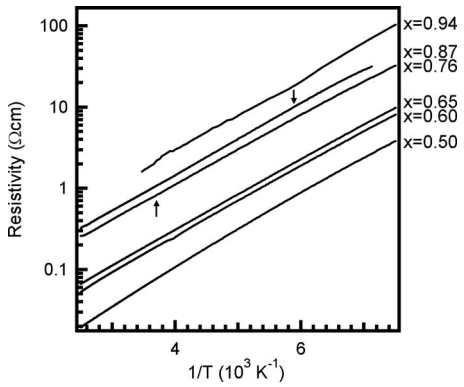

FIG. 6. Inverse temperature dependence of the electrical resistivities of $Fe_{2-x}Ti_xO_3$ films with various Ti concentrations x. The arrows indicate the Curie temperatures of the corresponding bulk crystals.

tration. Moreover, the resistivities of all films were lower than those of the corresponding bulk samples.[6] The activation energy E_{ac} for conduction was calculated using the formula $\rho=\rho_0 \exp(E_{ac}/kT)$. The obtained E_{ac} values were approximately 0.09 eV for all compositions, though the resistivity curves for $x=0.5$ appeared to be slightly inconsistent with the abovementioned simple formula. The E_{ac} value of 0.09 eV was also considerably smaller than that of the bulk ceramics (~0.2 eV).[6,21] The lower resistivity and smaller activation energy of the prepared films suggested their highly crystalline nature due to their epitaxial growth. Well-defined crystals with the (001) orientation should have high electrical conduction because of the predominant conductivity within the c plane.[22]

The charge carriers in both $FeTiO_3$ and α-Fe_2O_3 were regarded as small polarons.[21,23] The small activation energy required for the electrical conduction of $Fe_{2-x}Ti_xO_3$ films suggested the hopping of small polarons. However, the cation valence states in $Fe_{2-x}Ti_xO_3$ were very complicated. Two possible hopping paths—a homoatomic Fe^{2+}–Fe^{3+} path and a heteroatomic Fe^{2+}–Ti^{4+} path—should be considered. This could be a reason why the resistivity curves for $x=0.5$ showed composite behavior apart from the simple Arrhenius formula. The details of the hopping paths in the prepared $Fe_{2-x}Ti_xO_3$ films are discussed later. The magnetic transition in the $Fe_{2-x}Ti_xO_3$ films appeared to have no influence on their resistivities, though the T_C values of the films with $x=0.76$ and 0.87 were in the measured temperature range. The electrons hopping from Fe^{2+} to Fe^{3+} and/or Ti^{4+} strongly interacted with the surrounding lattices; the localized magnetic moments did not have any effect on the hopping electrons.

The electronic structures of the prepared $Fe_{2-x}Ti_xO_3$ films were examined by CEMS. Figure 7 shows the room temperature CEMS spectra of the $Fe_{2-x}Ti_xO_3$ films with various Ti concentrations. The films with high Ti concentrations, i.e., $x>0.7$, yielded the spectra of paramagnetic doublet patterns, while those with smaller concentrations, i.e., $x<0.7$, yielded magnetically split sextets. These results were fully consistent with those of the magnetization measurements. The magnetic ordering temperature of the $Fe_{2-x}Ti_xO_3$ films increased gradually with decreasing Ti concentrations across the room temperature at $x\sim0.7$. The broad components in

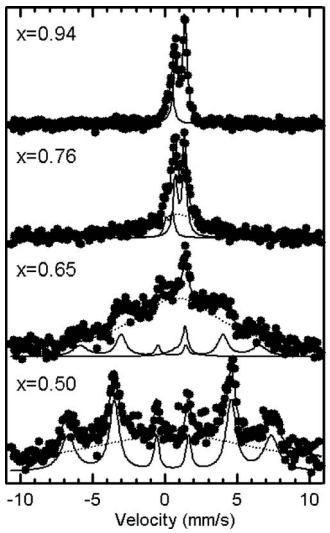

FIG. 7. Room temperature CEMS spectra of $Fe_{2-x}Ti_xO_3$ films with various Ti concentrations x.

the CEMS spectra were assigned to spin relaxation phenomena occurring because of thermally fluctuating electric and magnetic fields near the magnetic ordering temperature.[24]

It was difficult to accurately analyze the CEMS spectra near the magnetic ordering temperature because of the broadening and overlapping of peaks in the spectra. Therefore, the spectra were simply deconvoluted to assume the maximum three components including the broad background component. The fitted parameters for the spectra are listed in Table I. The CEMS spectrum of a (001)-oriented epitaxial $FeTiO_3$ film is known to have an asymmetric doublet with an intensity ratio of approximately 1:3 because the electric field gradient axis in $FeTiO_3$ coincides with the c axis.[13] The observed asymmetry in the doublet patterns for $x=0.94$ suggested the high crystallinity of the prepared films. The paramagnetic spectra consisted of two asymmetric doublets (labeled A and B in Table I). On the basis of their isomer shift (IS) values, components A and B were obviously as-

TABLE I. Fitted Mössbauer parameters for $Fe_{2-x}Ti_xO_3$ films shown in Fig. 7. "AV" indicates the averaged IS values of all components.

	Component	IS (mm/s)	Quadrupole splitting (mm/s)	Hyperfine field (kOe)	Relative area (%)
	A	1.06	0.64		79
$x=0.94$	B	0.33	0.35		21
		$(0.91)_{AV}$			
	A	1.04	0.63		31
	B	0.30	0.44		9
$x=0.76$	BG	0.78			60
		$(0.81)_{AV}$			
	A	1.11	0.58		4
	C	0.41		384	13
$x=0.65$	BG	0.82			83
		$(0.77)_{AV}$			
	C	0.43		436	28
$x=0.50$	BG	0.52			72
		$(0.49)_{AV}$			

signed to Fe^{2+} and Fe^{3+} ions, respectively.[25] The presence of individual Fe components with different valence states indicated that electron hopping between Fe^{2+} and Fe^{3+} ions did not occur beyond the Mössbauer time scale $\sim 10^{-7}$ s when the films had relatively high Ti concentrations, i.e., $x > 0.7$. On the other hand, when the Ti ions had tetravalent states, the chemical states of the films would be described as $Fe^{3+}_{0.12}Fe^{2+}_{0.94}Ti^{4+}_{0.94}O_3$. However, the $Fe^{3+}/(Fe^{2+}+Fe^{3+})$ ratio evaluated from the CEMS spectrum was 21%, which is considerably larger than that of the expected value (11%) from the above formula. One of the possible reasons for the large number of Fe^{3+} ions observed in $Fe_{2-x}Ti_xO_3$ was the oxygen nonstoichiometry that formed $Fe_{2-x}Ti_xO_{3+\delta}$. However, the unit cell volumes and magnetization measurements of the films suggested that the films had good stoichiometry. Another possible reason was the intervalence charge transfer such that $Fe^{2+}+Ti^{4+} \rightarrow Fe^{3+}+Ti^{3+}$. The electrical conductivity of $FeTiO_3$ was described by a hopping model of small polarons between Fe^{2+} and Ti^{4+} ions.[21] Moreover, the formation of Ti^{3+} states in $FeTiO_3$ because of the $Fe^{2+}+Ti^{4+} \rightarrow Fe^{3+}+Ti^{3+}$ charge transfer was also confirmed experimentally.[26] This could be a reason for the large $Fe^{3+}/(Fe^{2+}+Fe^{3+})$ ratio observed in the CEMS spectra of the $Fe_{2-x}Ti_xO_3$ films.

With a decrease in the Ti concentration, the averaged IS value for $Fe_{2-x}Ti_xO_3$ changed linearly from the one characteristic of Fe^{2+} ions to that of Fe^{3+} ions. The CEMS spectra of the films with $x < 0.7$ were analyzed by considering the magnetically split sextet pattern (labeled C). IS $=0.41-0.43$ mm/s obtained for component *C* was slightly larger than the IS values of typical Fe^{3+} ions, e.g., IS $=0.37$ mm/s in α-Fe_2O_3.[25] Fe ions assigned to component *C* should partially include the Fe^{2+} states in addition to the Fe^{3+} states. In the region $x < 0.7$, the Mössbauer spectra of the $Fe_{2-x}Ti_xO_3$ bulk samples[25] showed that a rapid electron transfer occurred between Fe^{2+} and Fe^{3+}. The formation of the mixed valence states between Fe^{2+} and Fe^{3+} could cause the low resistivities of the films. The predominant electron hopping path in $Fe_{2-x}Ti_xO_3$ appeared to switch from heteroatomic $Fe^{2+}-Ti^{4+}$ surroundings to homoatomic $Fe^{2+}-Fe^{3+}$ surroundings with decreasing Ti concentration.

IV. CONCLUSION

We have prepared well-crystallized epitaxial $Fe_{2-x}Ti_xO_3$ films on α-$Al_2O_3(001)$ single-crystalline substrates. All films with various Ti concentrations $0.5 < x < 1.0$ have the ordered ilmenite structure ($R\bar{3}$ symmetry). The structures and the magnetic and electric properties of the films have been systematically investigated as a function of the Ti concentration. All films have been formed epitaxially on the substrates, though the films are strained by a large amount, which causes tensile stress within the film plane. The known magnetic and electric properties of a bulk solid solution are essentially reproduced for thin films. Films with $x=0.5-0.7$ are ferrimagnetic at room temperature, and their electric resistivities are considerably small. The temperature dependence of the resistivities and the CEMS spectra suggest the conduction of small polarons hopping from Fe^{2+} sites to Ti^{4+} sites and from Fe^{2+} sites to Fe^{3+} sites, depending on the Ti concentration. The highly crystalline nature of the films and the formation of mixed valence states between Fe^{2+} and Fe^{3+} are the causes of the low resistivities of the films.

ACKNOWLEDGMENTS

The authors are grateful to Professor Z. Hiroi (University of Tokyo) for the measurement of the electric resistivity.

[1] H. Ohno, A. Shen, F. Matsukura, A. Oiwa, A. Endo, S. Katsumoto, and Y. Iye, Appl. Phys. Lett. **69**, 363 (1996).
[2] H. Ohno, J. Magn. Magn. Mater. **200**, 110 (1999).
[3] Y. Matsumoto, M. Murakami, T. Shono, T. Hasegawa, T. Fukumura, M. Kawasaki, P. Ahmet, T. Chikyow, S. Koshihara, and H. Koinuma, Science **291**, 854 (2001).
[4] Y. Ishikawa and S. Akimoto, J. Phys. Soc. Jpn. **12**, 1083 (1957).
[5] Y. Ishikawa, J. Phys. Soc. Jpn. **17**, 1835 (1962).
[6] Y. Ishikawa, J. Phys. Soc. Jpn. **13**, 37 (1958).
[7] W. H. Butler, A. Bandyopadhyay, and R. Srinivasan, J. Appl. Phys. **93**, 7882 (2003).
[8] A. Bandyopadhyay, J. Velev, W. H. Butler, S. K. Sarker, and O. Bengone, Phys. Rev. B **69**, 174429 (2004).
[9] N. C. Wilson, J. Muscat, D. Mkhonto, P. E. Ngoepe, and N. M. Harrison, Phys. Rev. B **71**, 075202 (2005).
[10] H. Hojo, K. Fujita, K. Tanaka, and K. Hirao, Appl. Phys. Lett. **89**, 082509 (2006).
[11] H. Hojo, K. Fujita, K. Tanaka, and K. Hirao, Appl. Phys. Lett. **89**, 142503 (2006).
[12] T. Fujii, M. Kayano, Y. Takada, M. Nakanishi, and J. Takada, Solid State Ionics **172**, 289 (2004).
[13] T. Fujii, Y. Takada, and J. Takada, Adv. Sci. Technol. (Faenza, Italy) **45**, 1309 (2006).
[14] Y. Takada, M. Nakanishi, T. Fujii, and J. Takada, J. Magn. Magn. Mater. **310**, 2108 (2007).
[15] R. W. Taylor, Am. Mineral. **49**, 1016 (1964).
[16] R. J. Harrison, S. A. T. Redfern, and R. I. Smith, Am. Mineral. **85**, 194 (2000).
[17] ICDD Powder Diffraction Files, $FeTiO_3$: 29–733, α-Fe_2O_3: 33–664.
[18] Y. Ishikawa and S. Akimoto, J. Phys. Soc. Jpn. **13**, 1110 (1958).
[19] N. E. Brown, A. Navrotsky, G. L. Nord, E. Dowty, and S. K. Banerjee, Am. Mineral. **78**, 941 (1993).
[20] F. Zhou, S. Kotru, and R. K. Pandey, Mater. Lett. **57**, 2104 (2003).
[21] B. Zhang, T. Katsura, A. Shatskiy, T. Matsuzaki, and X. Wu, Phys. Rev. B **73**, 134104 (2006).
[22] A. K. Mukerjee, Indian J. Phys. **38**, 10 (1964).
[23] K. Rosso, D. M. A. Smith, and M. Dupuis, J. Chem. Phys. **118**, 6455 (2003).
[24] B. N. Warner, P. N. Shive, J. L. Allen, and C. Terry, J. Geomagn. Geoelectr. **24**, 353 (1972).
[25] E. Murad and J. H. Johnston, in *Mössbauer Spectroscopy Applied to Inorganic Chemistry*, edited by G. J. Long (Plenum, New York, 1987), Vol. 2, p. 507.
[26] T. Fujii, M. Yamashita, S. Fujimori, Y. Saitoh, T. Nakamura, K. Kobayashi, and J. Takada, J. Magn. Magn. Mater. **310**, E555 (2007).